MOLECULAR AND CELLULAR BIOLOGY, Aug. 2007, p. 5352–5364 Vol. 27, No. 15
0270-7306/07/$08.00+0 doi:10.1128/MCB.00068-07

Conditional Deletion of Focal Adhesion Kinase Leads to Defects in Ventricular Septation and Outflow Tract Alignment▽†

Zeenat S. Hakim,[1] Laura A. DiMichele,[1] Jason T. Doherty,[1] Jonathon W. Homeister,[1,2] Hilary E. Beggs,[3,4] Louis F. Reichardt,[4,5] Robert J. Schwartz,[6] Joseph Brackhan,[1] Oliver Smithies,[1] Christopher P. Mack,[1,2] and Joan M. Taylor[1,2]*

Department of Pathology[1] and Carolina Cardiovascular Biology Center,[2] University of North Carolina, Chapel Hill, North Carolina 27599; Department of Opthamology,[3] Department of Physiology,[4] and Howard Hughes Medical Institute,[5] University of California, San Francisco, California 94143; and Institute of Biosciences and Technology, Houston, Texas 77030[6]

Received 12 January 2007/Returned for modification 20 February 2007/Accepted 17 May 2007

To examine a role for focal adhesion kinase (FAK) in cardiac morphogenesis, we generated a line of mice with a conditional deletion of FAK in *nkx2-5*-expressing cells (herein termed FAK^{nk} mice). FAK^{nk} mice died shortly after birth, likely resulting from a profound subaortic ventricular septal defect and associated malalignment of the outflow tract. Additional less penetrant phenotypes included persistent truncus arteriosus and thickened valve leaflets. Thus, conditional inactivation of FAK in *nkx2-5*-expressing cells leads to the most common congenital heart defect that is also a subset of abnormalities associated with tetralogy of Fallot and the DiGeorge syndrome. No significant differences in proliferation or apoptosis between control and FAK^{nk} hearts were observed. However, decreased myocardialization was observed for the conal ridges of the proximal outflow tract in FAK^{nk} hearts. Interestingly, chemotaxis was significantly attenuated in isolated FAK-null cardiomyocytes in comparison to genetic controls, and these effects were concomitant with reduced tyrosine phosphorylation of Crk-associated substrate (CAS). Thus, it is possible that ventricular septation and appropriate outflow tract alignment is dependent, at least in part, upon FAK-dependent CAS activation and subsequent induction of polarized myocyte movement into the conal ridges. Future studies will be necessary to determine the precise contributions of the additional *nkx2-5*-derived lineages to the phenotypes observed.

The heart is the first organ to form, and its development involves an intricate and complex series of events that must occur in a coordinated spatial and temporal fashion (44, 60, 75). The heart develops from bilaterally symmetric cardiogenic primordia that migrate and fuse at the embryonic midline to form a functional primitive heart tube that subsequently undergoes rightward looping to orient the atrial and ventricular chambers and properly align the outflow tract (OFT). As the chambers mature, the trabecular layer within the ventricles is elaborated, endocardial cushions form and fuse, and the chamber walls grow and thicken as the cardiomyocytes continue to proliferate and differentiate. A critical event in cardiac development related to human congenital heart defects (CHD) is septal morphogenesis, which commences during midgestation. The single ventricle becomes septated by a process involving fusion of the muscular interventricular septum (IVS) with the endocardial cushions, and further septation and valve formation continues until birth to ensure unidirectional flow of blood. Since multiple cell types, including those derived from the myocardium, endocardium, epicardium, and neural crest, contribute to the complex process of valvuloseptal morphogenesis, it is not surprising that CHD associated with aberrant septation of the OFT are quite common. Indeed, CHD afflict nearly 1% of newborn infants each year, and defective valvuloseptal morphogenesis is the leading cause of preterm mortality in the United States (22, 23, 53, 59). Thus, understanding the precise mechanisms underlying cardiac morphogenesis will aid in the identification of new therapies to target a multitude of congenital diseases (48).

Both forward and reverse genetic studies with *Drosophila melanogaster*, zebrafish, *Xenopus laevis*, and mice have been instrumental in determining the transcription factors required for vertebrate heart specification, patterning, and differentiation (42). Included in this growing list of key cardiac specification/differentiation transcription factors are Nk factors (cardioblast specification), MEF2 and GATA factors (cardiomyocyte differentiation), d- and e-Hand (right and left ventricle formation, respectively), and TBX factors (ventricular septation) (42). In spite of this wealth of information regarding the transcription factors that coordinate cardiac morphogenesis, the signaling mechanisms that regulate heart formation are only just beginning to be elucidated. Of note, fibroblast growth factor (FGF) signaling regulates mesodermal differentiation into cardiac primordia, BMPs (members of the transforming growth factor β2 [TGF-β2] superfamily) regulate cardioblast specification, cushion formation, and OFT septation, and the neuregulin growth factors ErbB2 and ErbB4 are required for the development of trabeculae (44).

Genetic evidence indicates that the integrin class of fibronectin-binding adhesion receptors ($\alpha_5\beta_1$ and others) can also regulate both the form and function of the heart (8, 21, 55, 56, 58, 66, 74). Integrin ligation drives the recruitment of a

* Corresponding author. Mailing address: Department of Pathology and Lab Medicine, 501 Brinkhous-Bullitt Bldg. CB 7525, University of North Carolina, Chapel Hill, NC 27599. Phone: (919) 843-5512. Fax: (919) 966-6718. E-mail: jmt3x@med.unc.edu.

† Supplemental material for this article may be found at http://mcb.asm.org/.

▽ Published ahead of print on 25 May 2007.

number of structural and signaling molecules to the ventral plasma membrane collectively termed a focal adhesion, which serves to link the force-generating actin cytoskeleton inside the cell to the extracellular matrix (ECM) and to coordinate the activation of downstream signaling pathways (28). The nonreceptor tyrosine kinase focal adhesion kinase (FAK) is strongly activated by both integrins and growth factors and is a likely candidate to integrate downstream signals from these diverse pathways during growth and development (50). FAK is expressed at relatively high levels in the mouse mesoderm at embryonic day 7.5 (E7.5) and continues to be expressed in the heart and several other tissues throughout adulthood (15). Germ line deletion of FAK resulted in mesodermal defects and embryonic lethality between E8.5 and E10. The *fak*$^{-/-}$ embryos showed a phenotype similar to that observed for both fibronectin- and α_5-null mice (30, 74). Although a rudimentary, nonbeating heart was apparent in some of these embryos, serial sectioning through *fak*$^{-/-}$ hearts revealed a lack of separate mesocardial and endocardial layers, which is indicative of defective cardiomyocyte maturation (15). Interestingly, germ line deletion of the FAK binding partners paxillin and Crk-associated substrate (CAS) also led to embryonic lethality associated with similar cardiac defects (19, 25). Paxillin and CAS are both adapter proteins that upon phosphorylation by FAK recruit additional signaling molecules to the focal adhesion complex and cause subsequent activation of downstream mitogen-activated protein kinase and GTPase-mediated signaling cascades (51). Taken together, these studies indicate that modulation of focal adhesion-dependent signals likely plays an important role in cardiac development and/or function.

In order to study the time- and tissue-dependent requirements for FAK in mouse development, Beggs et al. recently generated and characterized a mouse line (*fak*$^{flox/flox}$) in which exon 20 of the FAK gene (encoding the ATP binding domain) is flanked by loxP sites (3). We recently used this line to conditionally delete FAK from adult cardiomyocytes by use of a well-characterized *mlc2v*^{Cre} line. Somewhat surprisingly, we found that FAK is dispensable for basal cardiac function and myocyte viability. However, FAK was required for appropriate age- and pressure overload-induced compensatory myocyte hypertrophy. Indeed, mice with myocyte-restricted depletion of FAK had a blunted hypertrophic response that manifested in compromised heart function but not premature death (12). Herein, to determine whether FAK might play a direct role in cardiac morphogenesis, we generated a mouse with embryonic FAK deficiency in *nkx2-5*-expressing cells by use of a recently described Cre knock-in mouse line (46). We found that embryonic deletion of FAK in the *nkx2-5*-expressing cells results in perinatal lethality associated with a profound subaortic ventricular septal defect (VSD) and an abnormal OFT alignment. FAK inactivation does not affect myocyte growth or survival but regulates myocyte migration, a function that may play a role in the proper fusion of OFT cushion tissue with the muscular IVS.

MATERIALS AND METHODS

Antibodies. The anti-rabbit FAK antibody and the anti-mouse extracellular signal-regulated kinase 2 (anti-ERK2) antibody (1B3B9) were purchased from Upstate Biotechnology, Inc. The Pyk2 antibody was purchased from BD Transduction Laboratories, the laminin antibody was from Sigma, the Texas Red-conjugated phalloidin was purchased from Molecular Probes, and the anti-human phosphorylated Y410CAS antibody (which aligns with Y414 in mouse) was from Cell Signaling Technologies. The cardiac troponin T (cTNT) monoclonal antibody (13-11) was a gift from Nadia Malouf (UNC, Chapel Hill, NC), and the sarcomere myosin antibody (MF20) was purchased from the Developmental Studies Hybridoma Bank (University of Iowa).

Generation of mice. (i) FAK^{nk} mice. Louis Reichardt and Hilary Beggs (UCSF) provided the *fak*$^{flox/flox}$ mice, and Robert Schwartz (Institute of Biotechnology, Houston, TX) provided the *nkx2-5*^{Cre} knock-in mice (3, 46). Both lines of mice were backcrossed to the C57BL6 background for at least six generations prior to subsequent breeding. The breeding strategy entailed first breeding *fak*$^{flox/flox}$ mice with *nkx2-5*^{Cre} mice to generate *fak*$^{flox/wt}$ *nkx2-5*$^{Cre/wt}$ mice and subsequently mating the *fak*$^{flox/wt}$ *nkx2-5*$^{Cre/wt}$ mice with the *fak*$^{flox/flox}$ mice to obtain *fak*$^{flox/flox}$ *nkx2-5*$^{Cre/wt}$ (FAK^{nk}) mice.

(ii) *BGBP*$^{gfpX/gfpX}$ female and *BGBP*$^{gfpX/Y}$ male mice. A targeting construct was generated that contained a 3.2-kb rat cardiac beta myosin heavy chain (β-MHC) promoter fragment (a gift from Fadia Haddad, University of California Irvine, CA) upstream of the *Renilla reniformis* green fluorescent protein (GFP) (Stratagene) followed by another copy of the 3.2-kb rat cardiac β-MHC promoter region upstream of puromycin *N*-acetyltransferase (see Fig. S2 in the supplemental material). The reporter transgene was cloned into the hypoxanthine phosphoribosyltransferase-targeting vector, a modified version of pSKB1 (9). The targeting vector was linearized with PmeI before electroporation. Cell culture, electroporation, selection, and microinjection of embryonic stem cells were performed as described in reference 9. Female *BGBP*$^{gfpX/gfpX}$ mice were intercrossed with male *fak*$^{flox/flox}$ mice to generate homozygous female *fak*$^{flox/flox}$ *BGBP*$^{gfpX/gfpX}$ mice that were subsequently mated to male *fak*$^{flox/wt}$ *nkx2-5*$^{Cre/wt}$ mice to obtain embryos harboring GFP-positive cardiomyocytes with or without FAK deficiency (FAK$^{nk/gfp}$ and genetic control^{gfp}, respectively). All mice were maintained in a facility accredited by the Association for the Assessment and Accreditation of Laboratory Animal Care International according to Institutional Animal Care and Use Committee-approved guidelines. For timed matings, noon of the plug day was defined as E0.5. DNA isolated from tail snips, yolk sacs, or tissues was subjected to PCR analysis using primers specific for Cre and the presence of the targeted or recombined FAK allele as described previously (3, 76). The genotypes of the BGBP mice were determined by confirming the presence of GFP by PCR using primers 5′-GCG-ACT-TCT-TCA-TCC-AGA-GC-3′ and 5′-CCT-TGC-TCT-TCA-TCA-GGG-TGC-3′, and the absence of wild-type hypoxanthine phosphoribosyltransferase was confirmed using primers 5′-ATG-AAG-AAG-CGA-GCC-TTT-GGT-AA-3′ and 5′-AGT-TAC-AGG-GCA-TCC-CAA-TGT-TAC-3′.

Western blot analysis. Lysates were prepared from embryonic hearts or tissues as described previously (63). Antibodies for FAK, Pyk2, and ERK were used at a 1:1,000 dilution for immunoblot analysis, which was performed as previously described (63).

Histology. Embryos from timed matings were harvested at the desired stages of gestation. Embryonic tissues or embryos were fixed in 4% paraformaldehyde in phosphate-buffered saline (PBS), dehydrated, cleared, and embedded in paraffin. Morphological studies were carried out using transverse or coronal serial sections (8 to 10 μm) stained with hematoxylin-eosin, Mason's trichrome (Sigma), cTNT (1:100), laminin (1:100), or MF20 (1:10) antibodies using standard procedures.

Apoptosis and cell proliferation assays. Apoptosis was assessed for paraffin-embedded tissue sections by use of a DNA fragmentation detection kit, FragEL DNA (Calbiochem), according to the manufacturer's protocol. Cardiac cell proliferation was determined by bromodeoxyuridine (BrdU) labeling, which was achieved by administering 100 mg of BrdU (Sigma)/kg of body weight to pregnant mice intraperitoneally. Embryos were harvested an hour later, fixed, and embedded in paraffin. BrdU incorporation was detected by immunohistochemistry using a commercially available kit (Zymed). Apoptosis and cell proliferation were quantified by scoring the number of FragEL- and BrdU-positive nuclei in the muscular IVS per unit area by use of NIH Image J software.

Semiquantitative reverse transcription-PCR (RT-PCR). Hearts from E18.5 embryos were excised and stored in RNAlater (Ambion) at −80°C until RNA extraction. Samples were later homogenized, and RNA was extracted using TRIzol reagent (Invitrogen). cDNA was obtained by reverse transcription using a commercially available kit (iScript; Bio-Rad). PCR analysis of the cDNA was carried out using 2 μl of cDNA as a template and 0.5 μl of TaKaRa Ex *Taq* enzyme and previously published primers and cycling conditions. For primer sequences and references, see Table S1 in the supplemental material.

Transwell migration assay. Ventricles from E14.5 embryonic hearts were minced, rinsed extensively in PBS, and treated with 0.05% trypsin in PBS for 15

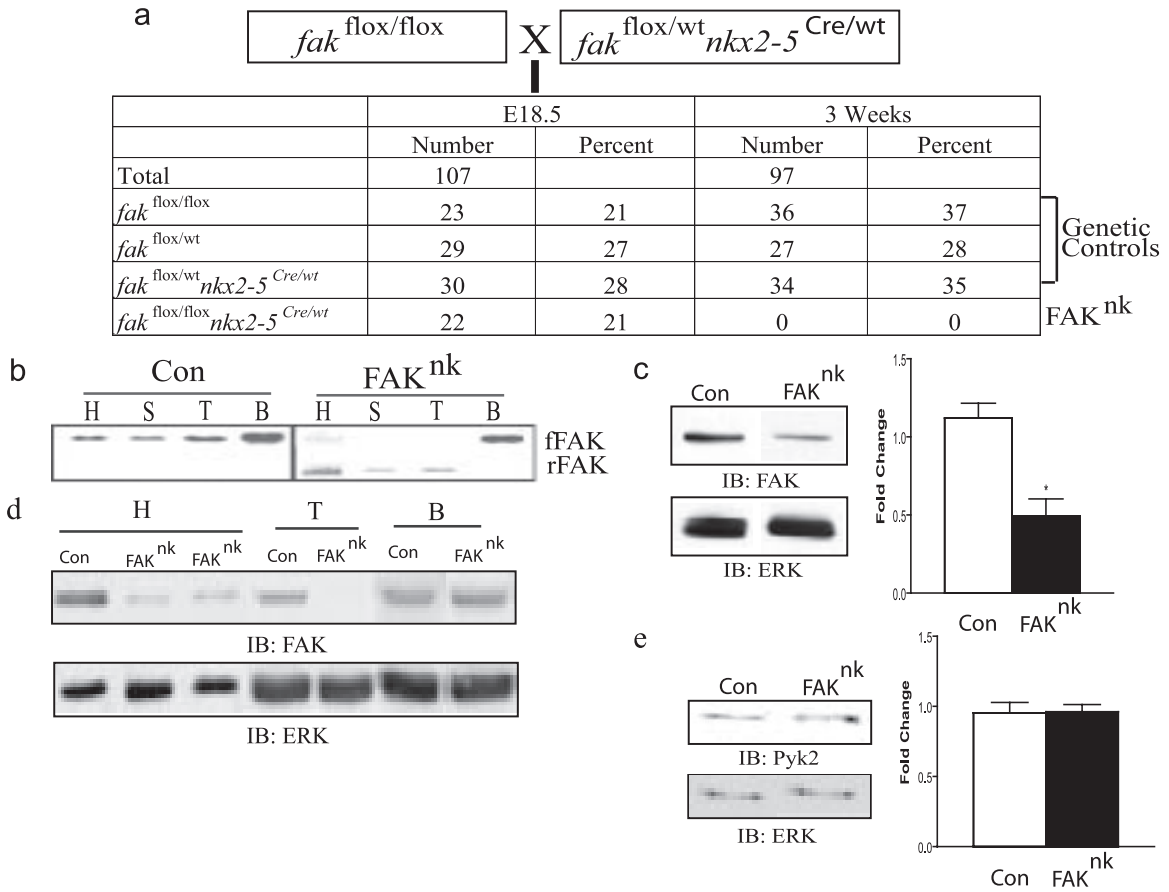

FIG. 1. Generation of FAK^{nk} mice. (a) Homozygous floxed FAK (*fak*$^{flox/flox}$) mice were bred with *nkx2-5*^{Cre} mice that were heterozygous for floxed FAK (*fak*$^{flox/wt}$ *nkx2-5*^{Cre}) to produce progenies with or without conditional deletion of FAK in *nkx2-5*-expressing cells. The progenies observed at E18.5 and 3 weeks are shown. (b) PCR analysis of DNA from heart (H), spleen (S), tongue (T), and brain (B). Primers specific for FAK recombination revealed a 350-bp band for recombined floxed FAK (rFAK) in the FAK^{nk} heart, spleen, and tongue. A 1.6-kb band for floxed FAK (fFAK) sequence (indicating lack of recombination) was present in the brain and to a much lesser extent in the heart in the FAK^{nk} mutants compared to the genetic controls (Con). (c) Western analysis of heart lysates at E13.5 revealed a significant decrease in the FAK levels in FAK^{nk} hearts compared to the genetic controls. Immunoblot (IB) (left) and densitometry quantification (right) of FAK protein levels compared to those of an ERK loading control ($n = 3$, $P < 0.05$). (d) Immunoblot of heart, tongue, and brain lysates from genetic control and FAK^{nk} mice at E18.5 probed with anti-FAK (top) and anti-ERK (bottom) antibodies. (e) (left) Immunoblot of protein extracts from E18.5 genetic control or FAK^{nk} hearts probed with anti-Pyk2 (top) or anti-ERK (bottom) antibodies; (right) densitometry quantification of Pyk2 expression compared to an ERK loading control ($n = 3$).

min at 37°C. The ventricle fragments were then triturated to obtain a single-cell suspension. Approximately 10,000 cells were resuspended in 300 μl of heart medium (Dulbecco's minimal essential medium plus M199 [4:1] containing 15% fetal bovine serum) and plated on transwell filters (8-μm pore size) precoated with fibronectin (10 μg/well). After 24 h, the adherent GFP-positive cells on the upper surface of the filter were counted in eight fields. The medium in the transwell chamber was replaced with serum-free heart medium, and the chamber was then placed in serum-containing medium to provide a chemoattractant gradient. Twenty-four hours later, the cells were fixed with 4% paraformaldehyde in PBS. The nonmigrated cells on the upper surface of the filter were removed with a cotton swab, the GFP-positive cells on the lower surface were counted, and the relative number of migrating cells was calculated.

Immunofluorescence. Cells were isolated from the embryonic hearts from E14.5 to E18.5 as described above and plated on fibronectin-coated chamber slides (10 μg/cc^3; Labtek). Cells were serum starved for 24 h and treated with phenylephrine (PE) (100 μM) or vehicle for 30 min. Cells were fixed with 4% paraformaldehyde in PBS for 20 min, rinsed with PBS, permeabilized with 0.4% Triton X-100 in PBS for 10 min, and incubated with 5% goat serum and 3% bovine serum albumin in PBS for 30 min to block nonspecific antibody binding. The cells were then incubated with Texas Red-conjugated phalloidin (1:1,000), anti-cTNT (1:1,000), anti-FAK (1:300), or anti-phospho-Y410CAS (1:300) antibodies in PBS for 1 h. The slides were washed with PBS, incubated with fluorescein isothiocyanate- or Texas Red-conjugated secondary antibodies, washed with PBS, and mounted with Vectashield (Vector Labs).

RESULTS

FAK deletion in *nkx2-5*-expressing cells. In order to study a role for FAK in cardiac morphogenesis, we crossed *fak*$^{flox/flox}$ mice to the *nkx2-5*^{Cre} line, in which the endogenous *nkx2-5* promoter drives Cre recombinase expression. This line of mice has been reported to induce Cre expression in cardiac progenitors at E7.5 and to induce recombination as early as E9 in cardiomyocytes (46, 73, 76). Consistent with the expression pattern of *nkx2-5*, this line induces recombination in cells within the anterior heart field (AHF), pharyngeal endoderm and ectoderm, spleen, tongue dorsum, tooth primordium, and stomach (29, 46, 73, 77). At E18.5, we found the appropriate Mendelian distribution of FAK^{nk} embryos; however, we did not find any FAK^{nk} mice upon weaning at 3 weeks of age

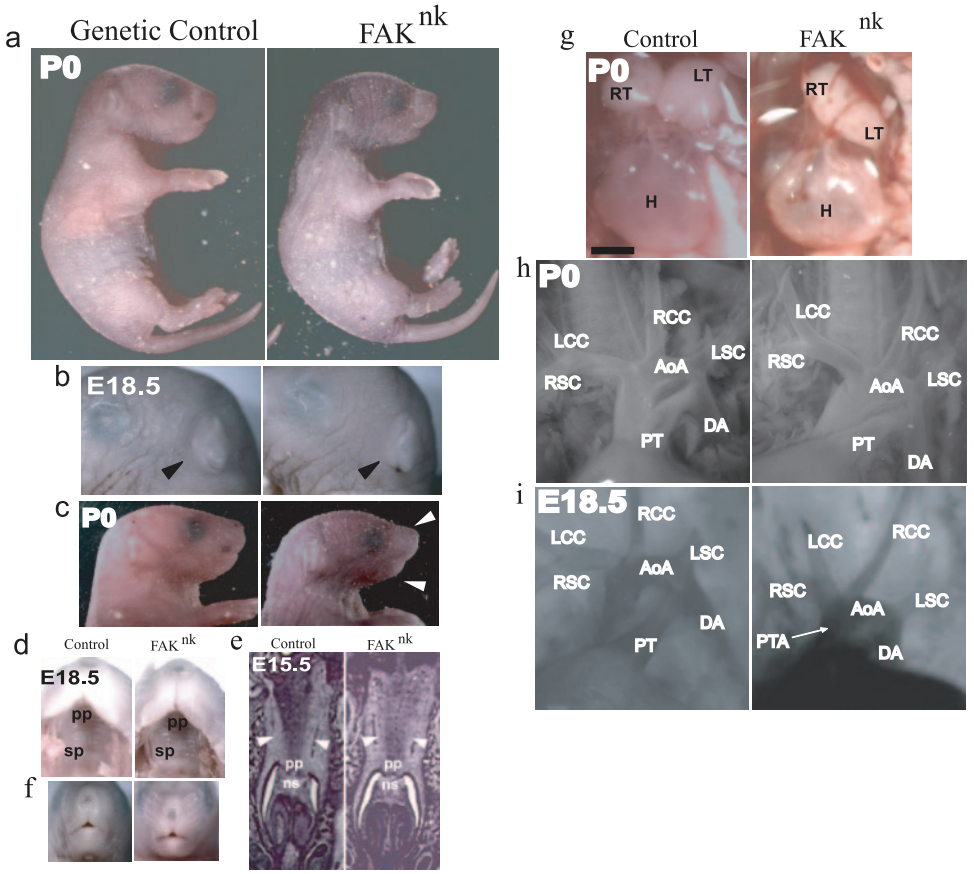

FIG. 2. Gross phenotypic analysis of FAK^{nk} mice. (a) The FAK^{nk} mutants appear fully developed at birth but are cyanotic. (b and c) FAK^{nk} mice (right) have normal external ears (black arrows) but slightly underdeveloped jaws (white arrows). (d to f) The FAK^{nk} embryos do not show cleft palate (d and e) or cleft face (f). Transverse sections of E15.5 embryos show fusion of the two palatal shelves (white arrows) and fusion of the nasal septum with the primary palate in the genetic control and FAK^{nk} embryos. (g) Postnatal FAK^{nk} thymus lobes are hypoplastic and the hearts are misshaped compared to what is seen for the genetic controls. (h) Most FAK^{nk} mutants (right) show a distinct aortic and pulmonary outflow emerging from the heart, suggesting proper aorticopulmonary septation. FAK^{nk} mutants showed normal arrangement of aortic branches from the outflow and the aortic arch in mutants with PTA. (i) Intracardiac injection of 0.5% Evans blue revealed that a fraction of the FAK^{nk} mutants present with PTA, indicative of impaired aorticopulmonary septation (right). AoA, aortic arch; DA, descending aorta; H, heart; LCC, left common carotid artery; LSC, left subclavian artery; LT, left lobe of the thymus; ns, nasal septum; pp, primary palate; PT, pulmonary trunk; RCC, right common carotid artery; RSC, right subclavian artery; RT, right lobe of the thymus; sp, secondary palate. Scale bar, 1 mm.

(Fig. 1a), suggesting that these mice survived in utero throughout gestation but died postnatally. Indeed, subsequent studies revealed that the FAK^{nk} neonates were born full term and appeared fully developed; however, they rapidly developed cyanosis and died within 10 to 120 min after birth (Fig. 2a). Each of the other genotypes generated from the crosses (*fak*$^{flox/flox}$ *nkx2-5*$^{wt/wt}$, *fak*$^{flox/wt}$ *nkx2-5*$^{wt/wt}$, or *fak*$^{flox/wt}$ *nkx2-5*$^{Cre/wt}$) were produced in the expected numbers and were viable, healthy, and fertile.

Contingent on coinheritance of *nkx2-5*^{Cre} and "floxed" FAK alleles, recombination occurred in the heart and other tissues that express *nkx2-5* (spleen and tongue) but not in brain, which does not express *nkx2-5* (Fig. 1b). Western analysis revealed that FAK protein levels were significantly reduced as early as E13.5 (Fig. 1c) and markedly reduced at E18.5 in the hearts of the FAK^{nk} embryos, compared to the genetic controls (Fig. 1d). At E18.5, FAK protein levels were also reduced in the tongue but not in the brain (Fig. 1d), consistent with the *nkx2-5* expression pattern during development. The low level of FAK protein remaining in the heart lysates is likely due to expression in resident nonmyocytes (i.e., cardiac fibroblasts and smooth muscle cells) that do not express *nkx2-5*. We found comparable levels (and activities) of the FAK-related protein Pyk2/CADTK in control and FAK^{nk} hearts (Fig. 1e and data not shown), indicating that Pyk2 likely does not compensate for the loss of FAK in this model.

Upon gross examination, the FAK^{nk} embryos (E18.5) or neonates (postnatal day 0 [P0]) were not strikingly different in external appearance from the genetic control littermates (Fig. 2a). The FAK^{nk} mice were similar in size and had normal limb and external ear development (Fig. 2a and b). In addition, the FAK^{nk} mice exhibited normal fusion of the secondary palatal shelves, and no incidence of cleft palate (Fig. 2d and e) or cleft face (Fig. 2f) was observed. However, the FAK^{nk} mutants did present with some abnormalities of other structures derived from the *nkx2-5*-expressing cells of the pharyngeal apparatus (PA). In particular, the FAK^{nk} mice had underdeveloped lower jaws (Fig. 2c), and both lobes of the thymus were hypo-

plastic in comparison to those of genetic control mice (Fig. 2g). While postnatal FAK^{nk} hearts appeared slightly distended in comparison to those of the genetic controls, examination of the OFT revealed that the arrangement of the aortic braches and the aortic arch appeared normal in most FAK^{nk} mutants (Fig. 2g and h). However, a fraction (4/32) of the FAK^{nk} mice did present with incomplete aorticopulmonary septation and persistent truncus arteriosus (PTA) as assessed by Evans blue dye injection (Fig. 2i).

Since *nkx2-5*^{Cre} is also expressed in the spleen, tongue, and stomach (46), we examined these organs histologically to evaluate potential developmental abnormalities that in theory could contribute to the demise of FAK^{nk} neonates. The gastric anatomy, including histologic cell types, was intact and consistent between genotypes (data not shown). Similarly, the gross and histologic structures of the tongue were not altered in FAK^{nk} neonates. Spleens of FAK^{nk} neonates grossly were small and appeared pale compared to spleens from the genetic controls, but histologically they appeared similar (data not shown). The lack of gross and histologic abnormalities in these organs in conjunction with the progressive cyanosis and death of the P0 neonates within minutes of birth indicates that CHD is likely the proximate cause of death.

FAK regulates ventricular septation and OFT alignment. We performed a histological analysis of FAK^{nk} ($n = 32$) and littermate genetic control (*fak*$^{flox/flox}$ *nkx2-5*$^{wt/wt}$ [$n = 24$] or *fak*$^{flox/wt}$ *nkx2-5*$^{Cre/wt}$ [$n = 18$]) hearts at selected time points ranging from E12.5 to P0 to further characterize the cardiac defects. At E18.5, the gross size and structure of most FAK^{nk} hearts appeared normal (13 of 16 hearts) relative to the genetic controls, while the remaining 3 hearts were slightly reduced in size (compare Fig. 3a and b with c and d). However, most postnatal (P0) FAK^{nk} hearts ($n = 4$) did appear malformed histologically, possibly as a result of abnormal postnatal hemodynamic changes in these hearts (compare Fig. 3e with f and g). Histological analysis revealed a profound subaortic membranous VSD in 24 of 27 FAK^{nk} hearts examined. There was no apparent hypoplasia of the right ventricle in these mutants and there appeared to be correct development of the OFT; however, the aortic side of the proximal OFT communicated with both left and right ventricles, resulting in an overriding aorta (OA) in 21/27 FAK^{nk} hearts (Fig. 3c, d, f, and g), while in 3 of 27 FAK^{nk} hearts both great vessels arose entirely from the right ventricle, resulting in a double-outlet right ventricle (DORV) (Fig. 3i). As noted above, most (25/32) FAK^{nk} mutants showed adequate septation of the truncus into the pulmonary and aortic trunks (Fig. 2g, right, and 3i), but a fraction (4/32) also demonstrated PTA with a complete lack of septation between the two OFTs (Fig. 2h, right, and 3n; also see Table 1).

Most of the FAK^{nk} hearts appeared to have normal atrioventricular (AV) valve development (Fig. 3k) and atrial septation (Fig. 3m), with the exception of one that showed a lack of contact of the mitral and tricuspid valve leaflets with the crest of muscular IVS (data not shown). The aortic valves were properly formed and appeared normal in most FAK^{nk} hearts; however, a fraction (4/27) of the FAK^{nk} hearts showed thickened semilunar valve leaflets (Fig. 3g). Trabeculae were formed in the FAK^{nk} hearts, indicating that FAK is not essential for this neuregulin-1/ErbB2/ErbB4-dependent process even though previous reports indicate that neuregulin-1 induces Src activity and complex formation between ErbB2, FAK, and Src in several cell types, including adult cardiomyocytes (4, 39, 65, 69). Compaction of the ventricular chambers was also relatively unaffected in most FAK^{nk} hearts, indicating that FAK is dispensable for myocyte maturation and cell-cell interactions. Importantly, we found no evidence of any morphogenetic defects in the 42 genetic control hearts examined from E12.5 to P0 (Fig. 3a, b, e, h, j, and l).

FAK^{nk} hearts exhibit abnormal OFT cushion morphogenesis. Ventricular septation depends upon proper formation of the muscular portion of the IVS as well as proper development of the endocardial cushions in the OFT and the AV canal, which undergo complex morphogenetic steps before fusing with the muscular IVS. To identify the cause of VSD and OA in the FAK^{nk} hearts, we examined embryos at E12.5 and E13.5, when the final stages of septation occur. Cushion morphogenesis appeared normal in the FAK^{nk} hearts at E12.5 (Fig. 4a to c). The aorta was anterior to the right ventricular OFT (Fig. 4a), and the endocardial cushions had developed in the OFT (Fig. 4b) and the AV canal (Fig. 4c). Myocyte-derived structures also appeared normal; the muscular IVS had grown toward the AV endocardial cushions (Fig. 4c) and the trabeculae showed similar patterns in the ventricles of the FAK^{nk} and control hearts (Fig. 4c). At E13.5, the OFT endocardial cushions appeared grossly normal and had fused along the midline in the proximal OFT in FAK^{nk} hearts (Fig. 4d, right). However, the conal ridges in the proximal OFT fused abnormally with the muscular IVS in the FAK^{nk} hearts (Fig. 4e, right), causing the aortic OFT to maintain contact with the right ventricle and resulting in OA or DORV in these hearts (Fig. 4f, right).

Since previous studies (52, 68) have revealed that myocardialization of the endocardial cushions is important for proper fusion of the OFT to the muscular IVS, we analyzed the cellular composition of the OFT cushions in control and FAK^{nk} hearts. At E13.5, a large number of MF20-positive cardiomyocytes were apparent in the septal and parietal conal ridges of the proximal OFT in the genetic control hearts (Fig. 5, top). However, there was a marked reduction in the MF20-positive cells in the OFT cushions of FAK^{nk} hearts (Fig. 5, bottom).

FAK deficiency in the *nkx2-5*-expressing cells does not alter proliferation, survival, or expression of important regulatory genes. The finding that the overall size of most FAK^{nk} hearts was comparable to that of litter-matched genetic control hearts indicates that generalized myocyte hypoplasia likely was not occurring in the FAK^{nk} hearts. However, we reasoned that the temporal deletion of FAK at E13.5 could lead to a selective growth or survival defect in the muscular IVS or endocardial cushions, which are undergoing extensive remodeling at this point in development. To address this question, we first examined the extent of apoptosis in control and FAK^{nk} hearts. As expected, numerous FragEL-positive cells were detected in the genetic control hearts at E13.5 in the OFT (Fig. 6a, top left) and AV (Fig. 6a, middle left) endocardial cushions as well as in the IVS (Fig. 6a, bottom). However, there was no significant difference in cell death levels between FAK^{nk} (Fig. 6a, right, and d) and genetic control (Fig. 6a, left, and d) hearts. Lower overall levels of FragEL-positive apoptotic cells were detected at E18.5, but still no significant difference was found between the FAK^{nk} hearts and those of the genetic controls (data not shown). This finding was substantiated by Western analysis to

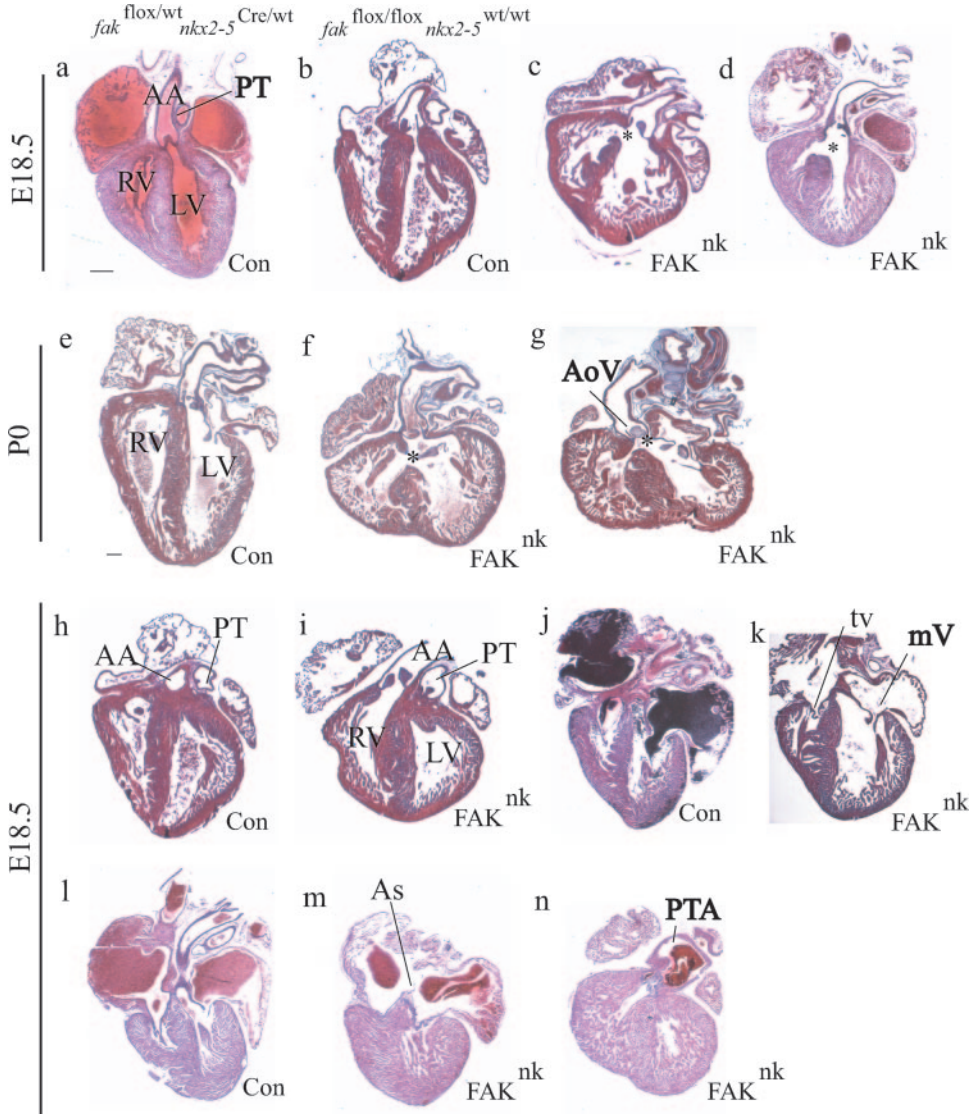

FIG. 3. FAK deficiency in *nkx2-5*-expressing cells results in defective ventricular septation and OFT alignment. Isolated hearts sectioned and stained with Mason's trichrome or hematoxylin and eosin. (a, b, e, h, j, and l) E18.5 and P0 genetic control hearts appear normal and do not show septation defects. (c, d, f, and g) FAK^{nk} hearts at E18.5 and P0 display a large, subaortic membranous VSD, as indicated by *. (g) FAK deficiency results in thickened and malformed aortic semilunar valves in some FAK^{nk} hearts. (i) Example of a FAK^{nk} heart that shows DORV with the aorta rising completely from the right ventricle. (k) Most FAK^{nk} hearts showed normal AV valves and (m) atrial septation. (n) Example of PTA in a FAK^{nk} heart. AA, ascending aorta; As, atrial septum primum; LV, left ventricle; mV, mitral valve; PT, pulmonary trunk; RV, right ventricle; tv, tricuspid valve; AoV, aortic semilunar valve; Con, control. Scale bar, 200 μm.

TABLE 1. Summary of phenotypes in late-term (E18.5) and P0 FAK^{nk} mutants

Phenotype	No. of mice		Penetrance (%)
	Examined	With phenotype	
Subaortic VSD	27	24	89
With OA	27	21	78
With DORV	27	3	11
PTA	32	4	13
AV valve defects	27	1	4
Semilunar valve hyperplasia	27	4	15

detect full-length and cleaved caspase 3 in E18.5 embryonic heart lysates. As shown in Fig. 6b, total caspase 3 protein levels were not significantly different between the genetic control and FAK^{nk} hearts, and very little cleaved caspase 3 was detected in either genotype, in accord with our findings that basal apoptosis is low at this embryonic time point. We also examined the expression levels of the apoptotic markers Bcl2 and Bax by semiquantitative RT-PCR at E18.5 and found that the levels (and ratios) of these genes were not significantly different between the FAK^{nk} and genetic control hearts (data not shown). Taken together, these data indicate that FAK is not necessary for embryonic myocyte survival and corroborate our previously published results that deletion of FAK from adult

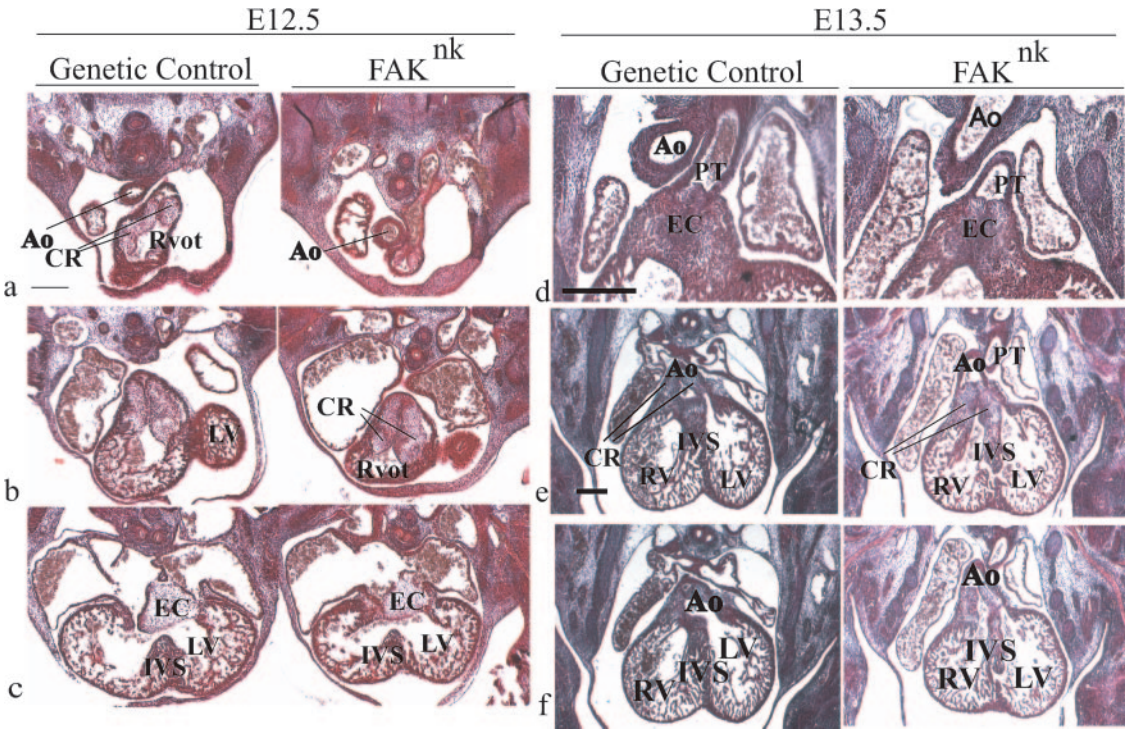

FIG. 4. FAK is essential for normal OFT cushion morphogenesis. Mason's trichrome or hematoxylin-eosin-stained sections from control and FAK^{nk} embryos at E12.5 and E13.5. (a) At E12.5, the aortic OFT was anterior to and to the right of the right ventricular OFT in the FAK^{nk} hearts. (b) The endocardial cushions appear normal in the OFT in the FAK^{nk} hearts at E12.5. (c) The AV canal endocardial cushions, the muscular IVS, and the trabeculae appear normal in the FAK^{nk} hearts (right) compared to genetic controls (left) at E12.5. (d) At E13.5, the conal ridges had proliferated and fused along the midline in the distal OFT in the genetic control (left) and FAK^{nk} (right) hearts. (e) At E13.5, the conal ridges had fused normally in the proximal OFT with the muscular IVS in the genetic control hearts (left), but this fusion was abnormal in the FAK^{nk} hearts (right). (f) At E13.5, the aorta maintained contact with the left ventricle in the genetic control hearts (left), but in the FAK^{nk} hearts, the aorta maintained contact with the right ventricle (right). Ao, aorta; CR, conal ridges; EC, endocardial cushion; LV, left ventricle; mV, mitral valve; PT, pulmonary trunk; Rvot, right ventricular OFT; RV, right ventricle; tv, tricuspid valve. Scale bars, 100 μm.

myocytes does not induce myocyte apoptosis or affect myocyte viability (12).

To determine whether depletion of FAK decreases cardiomyocyte proliferation in the affected region, we analyzed BrdU incorporation in FAK^{nk} and genetic control hearts at E13.5 and E18.5. We found that the numbers of BrdU-labeled cells in either the muscular IVS, the endocardial cushion tissue, or the ventricles of FAK^{nk} hearts did not differ significantly from those in the genetic controls (Fig. 6c and e and data not shown). Taken together, these data indicate that incomplete ventricular septation likely was not due to defective myocyte growth in the FAK^{nk} hearts.

It is clear that the initial stages of heart development, including myocyte specification and cardiac looping, were not affected in the FAK^{nk} hearts. However, since cardiomyocyte maturation continues throughout embryonic development, we examined whether the expression of myocyte-restricted differentiation markers might be altered in the FAK^{nk} hearts. Immunohistochemical analysis revealed that cTNT expression was unaltered in FAK^{nk} hearts in comparison to genetic control hearts at E18.5 (see Fig. S1a in the supplemental material). In addition, no significant differences in transcript levels for cardiac markers of differentiation (GATA4, MEF-2C, α-MHC), chamber specification (d-Hand), or ventricular septation (Tbx1 and Tbx5) were observed for FAK^{nk} hearts compared to genetic controls at E18.5, as assessed by RT-PCR (see Fig. S1b in the supplemental material). Since OFT defects have been associated with defective TGF-β2 signaling, we also examined expression of this growth factor, but we did not detect a significant difference in TGF-β2 expression in the FAK^{nk} hearts compared to the genetic controls (see Fig. S1 in the supplemental material). Gene expression of each of these markers of cardiac morphogenesis was comparable in the genetic controls used in this study, namely, *fak*$^{flox/flox}$ *nkx2-5*$^{wt/wt}$ and *fak*$^{flox/wt}$ *nkx2-5*$^{Cre/wt}$ (data not shown), indicating that neither the deletion of FAK nor the haploinsufficiency of *nkx2-5* leads to altered expression of these genes. It should be noted that the expression of *nkx2-5* was reduced by approximately 50% in FAK^{nk} hearts from the levels seen for the *fak*$^{flox/flox}$ *nkx2-5*$^{wt/wt}$ controls as expected, due to the haploinsufficiency of *nkx2-5* in our model, but the levels were comparable to those seen for stage-matched *fak*$^{flox/wt}$ *nkx2-5*$^{Cre/wt}$ embryonic hearts, indicating that FAK deletion does not alter *nkx2-5* transcription (data not shown). Thus, reduced dosage of *nkx2-5* likely does not account for the septal and OFT defects observed for the FAK^{nk} mice.

FAK^{nk} cardiac myocytes show reduced migration in vitro. The initial stage of myocardialization of the OFT is thought to involve the migration of cardiomyocytes from the flanking myocardium into the cushion mesenchyme (52, 68). To deter-

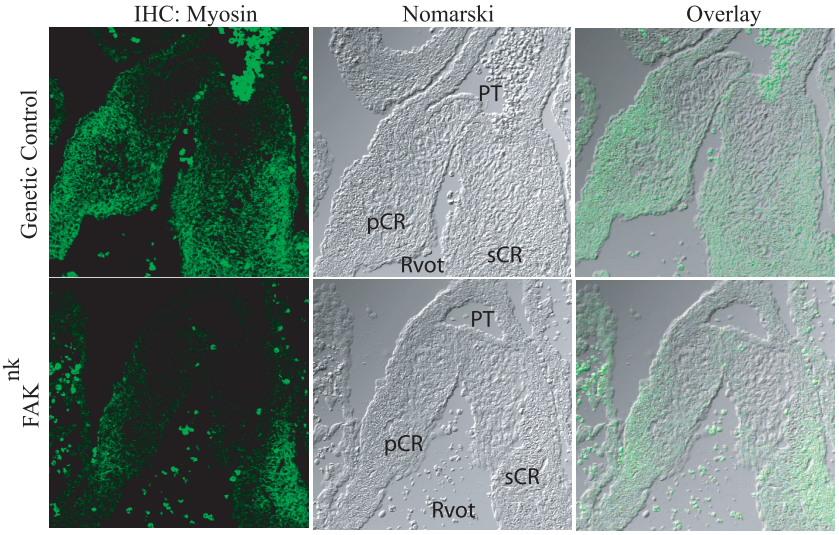

FIG. 5. FAK deficiency in *nkx2-5*-expressing cells impairs myocardialization of the OFT cushion tissue. Sections of the proximal OFT in genetic control and FAK^{nk} hearts stained with anti-sarcomere myosin antibody (MF20) at E13.5. The left panels show MF20 immunostaining (immunohistochemistry [IHC]), the middle panels show Nomarski images of the same views, and the right panels are overlays of the corresponding left and middle panels. A large number of MF20-positive cardiomyocytes were seen extending into the septal and parietal conal ridges of the proximal OFT from the underlying myocardium in the genetic control hearts at E13.5 (top). The numbers of cardiomyocytes were markedly reduced in the FAK^{nk} hearts in both conal ridges at E13.5 (bottom). pCR, parietal conal ridge; PT, pulmonary trunk; Rvot, right ventricular OFT; sCR, septal conal ridge.

mine whether impairment in cell-matrix interactions might contribute to the impaired myocardialization observed for the FAK^{nk} cardiomyocytes, we examined basal lamina organization in control and FAK^{nk} hearts. We found that the distribution and localization of laminin, an important ECM protein that plays a significant role in myocyte-ECM interactions, was unaltered in the muscular IVS in FAK^{nk} hearts at E13.5 (Fig. 6f).

We next used an in vitro approach to determine whether cardiomyocyte chemotaxis was regulated by FAK activity. Our initial experiments using either isolated cells or cardiac explants from FAK^{nk} and genetic control hearts proved problematic in distinguishing myocytes from nonmyocytes in three-dimensional migration assays. To overcome this hurdle, we crossed the *fak*$^{flox/flox}$ and *nkx2-5*^{Cre} mice to a novel line of mice in which nucleus-targeted GFP and the puromycin resistance transgenes are expressed under the control of a truncated β-MHC promoter (see Fig S2 in the supplemental material). FAK-containing and FAK-null cardiomyocytes isolated from these mice (designated as genetic control^{gfp} and FAK$^{nk/gfp}$, respectively) were identified by nuclear GFP expression, and these cells exhibited comparable well-defined sarcomeric actin organizations (Fig. 7a, left) and showed strong expression of cTNT (Fig. 7a, middle). Both cardiomyocytes and nonmyocytes derived from the genetic control^{gfp} hearts express high levels of FAK, which localized to focal adhesion structures at the periphery of cells. As expected, myocytes isolated from FAK$^{nk/gfp}$ mice revealed undetectable FAK immunoreactivity, while nonmyocytes (i.e., GFP-negative cells) isolated from the FAK$^{nk/gfp}$ hearts, which were likely cardiac fibroblasts, did express FAK (Fig. 7a, right). We next utilized these GFP-targeted cells to examine cardiomyocyte migration in vitro by using the Boyden transwell system. As shown in Fig. 7b, 15% serum stimulated a robust chemotactic response in cardiomyocytes isolated from genetic control^{gfp} hearts, while chemotaxis was dramatically reduced in FAK$^{nk/gfp}$ cardiomyocytes.

One candidate migratory pathway that could be regulated in a FAK-dependent fashion is the CAS/CRK/Rac pathway. Tyrosine phosphorylation of CAS on YXXP tyrosines within the CAS substrate domain creates binding sites for the SH2 domain of the adapter protein CRK. Recruitment of CRK to focal adhesions can in turn induce Rac activation and promote chemotaxis (7, 10, 37, 40, 61, 71). We previously reported that PE stimulated a rapid increase in total tyrosine phosphorylation of FAK and CAS in neonatal cardiomyocytes (64). Thus, we first examined whether PE could stimulate cardiomyocyte-associated CAS phosphorylation on a specific tyrosine (Y414 in mouse) which can direct CRK binding (57). As shown in Fig. 8, PE-induced striking phosphorylation of CAS on Y414 in distinct peripheral complexes in both cardiomyocytes and fibroblasts isolated from genetic control^{gfp} hearts following PE treatment (Fig. 8, top). The pY414CAS-decorated complexes were associated with myocyte membrane protrusions that are reminiscent of classical lamellipodial structures observed for migrating fibroblasts. Although PE stimulated Y414CAS phosphorylation in fibroblasts isolated from FAK$^{nk/gfp}$ hearts, the FAK-null cardiomyocytes lacked significant Y414CAS phosphorylation (Fig. 8, bottom). Similarly, treatment with serum induced pY414CAS phosphorylation in control but not in FAK-null cardiomyocytes (data not shown). Thus, FAK-deficient myocytes have reduced agonist-stimulated motility and agonist-stimulated phosphorylation of the promotile adapter protein CAS. These data imply that incomplete myocardialization and lack of subsequent ventricular septation in FAK^{nk} hearts may be due, at least in part, to defective polarized myocyte movement into the conal ridges.

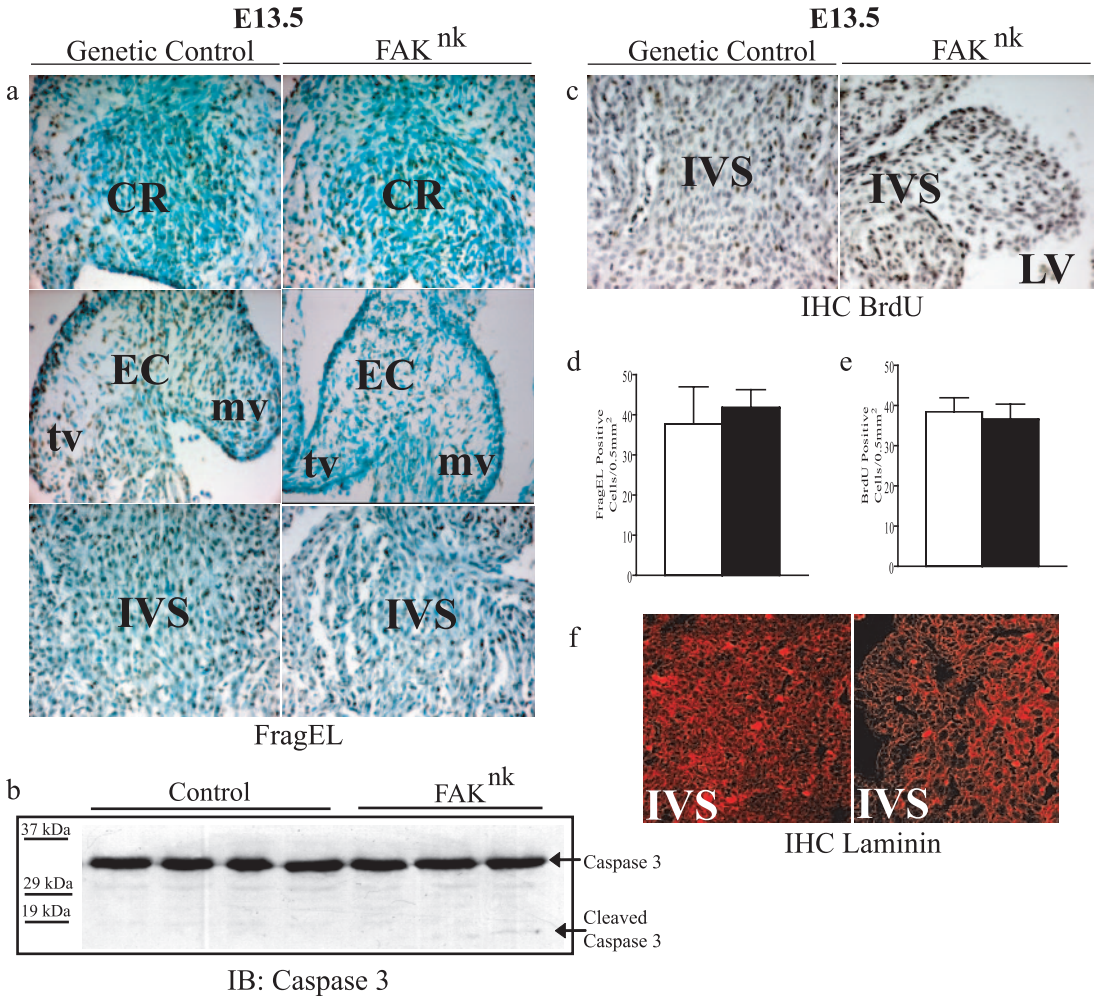

FIG. 6. FAK deficiency does not alter myocyte proliferation or survival. (a) FragEL staining of apoptotic cells of the proximal conal ridges in the OFT (top), the valve primordia (middle), and the muscular IVS (bottom) of genetic control and FAK^{nk} hearts at E13.5. Sections were counterstained with methyl green, and FragEL-positive nuclei appear brown as assessed by DAB (3,3′-diaminobenzidine) staining. (b) Western analysis (immunoblot [IB]) of total and cleaved caspase 3 levels in genetic control and FAK^{nk} hearts at E18.5. (c) BrdU incorporation in the muscular IVS in genetic control and FAK^{nk} hearts at E13.5. Sections were counterstained with hematoxylin, and BrdU-positive nuclei appear brown, as assessed by DAB staining. (d) Data represent mean ± standard error of FragEL-positive cells in 0.5 mm^2 of the muscular IVS area from three or four hearts ($P < 0.05$). (e) Data represent mean ± standard error of BrdU-positive cells in 0.5 mm^2 of the muscular IVS area from three or four hearts ($P < 0.05$). For panels d and e, white bars are for genetic control hearts, and black bars are for FAK^{nk} hearts. (f) High-power (magnification, ×40) images of the muscular IVS in genetic control and FAK^{nk} hearts stained with an anti-laminin antibody at E13.5. CR, conal ridges; EC, endocardial cushion; mv, mitral valve; tv, tricuspid valve.

DISCUSSION

Germ line deletion of FAK results in early embryonic lethality, making it difficult to study the specific role for FAK in cardiac development. To overcome this hurdle, we used the Cre-loxP system to induce conditional FAK deficiency in *nkx2-5*-expressing cells. Somewhat surprisingly, anabolic heart growth and most morphogenetic processes occurred normally in FAK-depleted hearts. However, FAK deletion in the *nkx2-5*-expressing cells caused malformations in the OFT that manifested as a profound subaortic VSD with OA or DORV, which were incompatible with postnatal life, most likely due to defective blood oxygenation. Additional notable (albeit less penetrant) phenotypes included defective conotruncal septation leading to PTA and thickened valve leaflets. Thus, conditional inactivation of FAK in the *nkx2-5*-expressing cells leads to the most common CHD that is also a subset of abnormalities associated with tetralogy of Fallot and the DiGeorge syndrome. The normal body and heart sizes of E18.5 FAK^{nk} embryos excluded generalized growth or function defects in the fetal FAK^{nk} hearts. Accordingly, proliferative and apoptotic cell indices were not significantly changed in the embryonic FAK^{nk} hearts in comparison to those of genetic controls. However, FAK deficiency in the *nkx2-5*-expressing cells did impair myocardialization of the conal ridges in the proximal OFT and significantly reduced myocyte migration in vitro, suggesting that impaired cardiomyocyte migration in the developing OFT could be one cause of the membranous VSD and OFT malalignment in the FAK^{nk} mice.

Since *nkx2-5* expression is not limited to the primary heart field, it is possible that deletion of FAK from nonmyocytes in

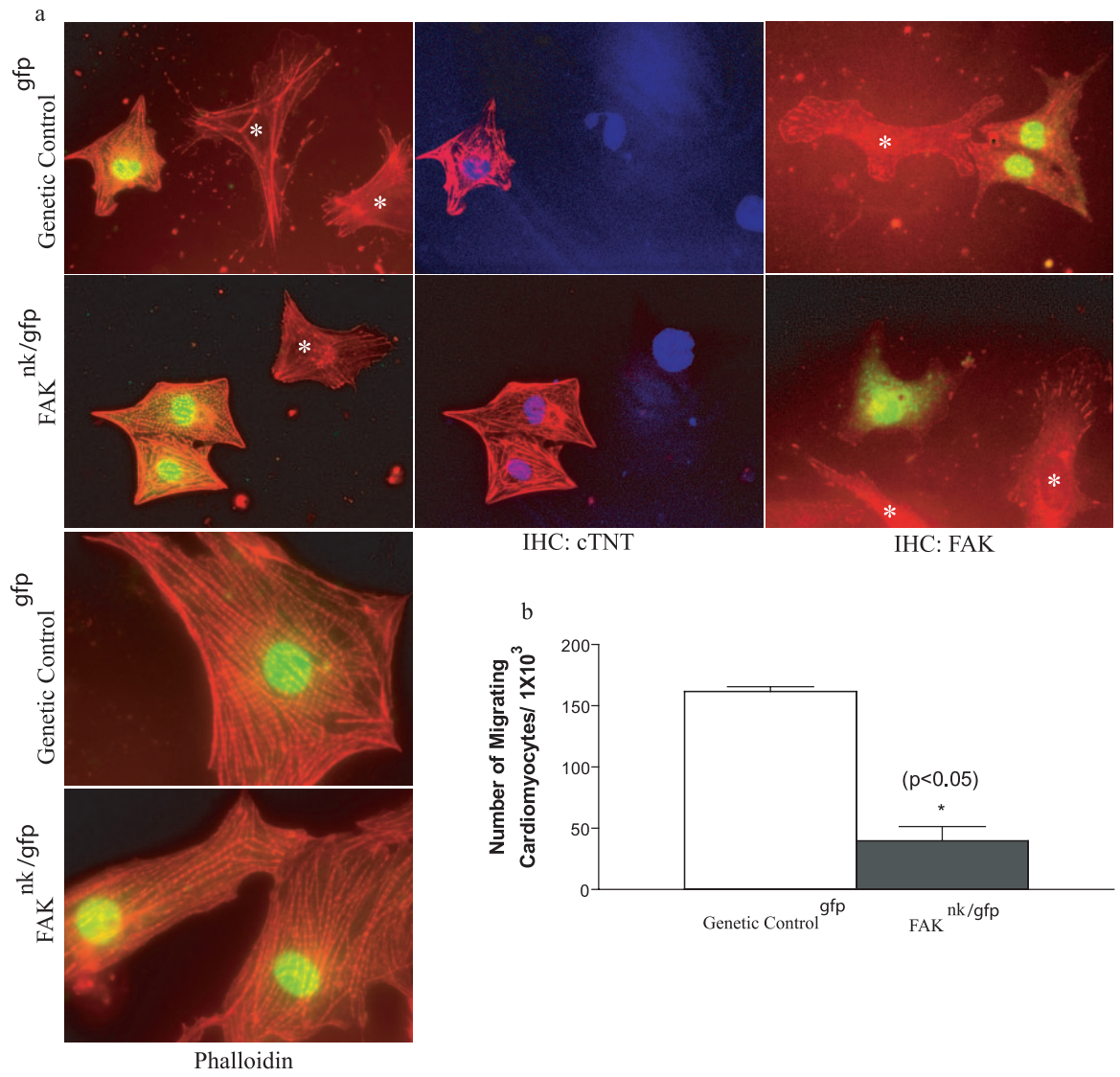

FIG. 7. Depletion of FAK does not affect myofibrillar organization but impairs cardiomyocyte motility. (a) Cells were isolated from genetic control^{gfp} and FAK$^{nk/gfp}$ hearts and processed for immunohistochemistry (IHC) as described in Materials and Methods. GFP-positive cells from the genetic control^{gfp} and FAK$^{nk/gfp}$ hearts showed a characteristic striated pattern of sarcomeric actin, as revealed by phalloidin staining (left), and high levels of cTNT (middle), as determined by immunohistochemistry. GFP-negative cells (*) are likely cardiac fibroblasts. Cells were also stained with anti-FAK antibodies to reveal the presence or absence of FAK in both myocytes and nonmyocytes (*) isolated from the genetic control^{gfp} and FAK$^{nk/gfp}$ hearts (right). (b) GFP-positive cells isolated from genetic control^{gfp} and FAK$^{nk/gfp}$ hearts were plated on Boyden chambers coated with fibronectin (10 μg/ml) as described in Materials and Methods. The data are presented as the mean number of GFP-positive migrating cells compared to the total of GFP-positive attached cells (± standard deviation) counted prior to addition of the chemoattractant (15% serum). The data are representative of cardiomyocytes isolated from three separate hearts from each genotype.

the AHF, pharyngeal endoderm, and first pharyngeal arch ectoderm and/or from cells derived from these regions could contribute to the phenotypes observed. Importantly, studies have indicated that abnormal development of cells within the AHF can manifest in septations and OFT defects similar to those observed for the FAK^{nk} mice (29, 70, 73). Cardiac neural crest cells (NCCs) also play an important role in the development of the pharyngeal arch arteries and septation of the OFT (1, 5, 34, 35, 47, 72). The cardiac NCCs migrate from their origin in the cranial folds to populate the third, fourth, and sixth pharyngeal arch arteries (PA), resulting in the expansion and development of the PA, which is crucial for OFT septation and aortic arch patterning (1, 33, 36, 62). Although we would not expect FAK to be depleted in the NCCs of the FAK^{nk} hearts (since *nkx2-5* is not expressed in NCCs), we cannot exclude the possibility that the depletion of FAK in the AHF and PA leads (indirectly) to defective NCC migration and/or survival, since it has been suggested that the AHF and NCCs may be functionally interdependent (17, 29). Indeed, the malformation of the lower jaw and the thymic hypoplasia as well as the less penetrant PTA phenotype observed for FAK^{nk} mice were likely due to defective NCC function that may have resulted from the ablation of FAK in the PA in early development. Future studies using additional Cre lines coupled with

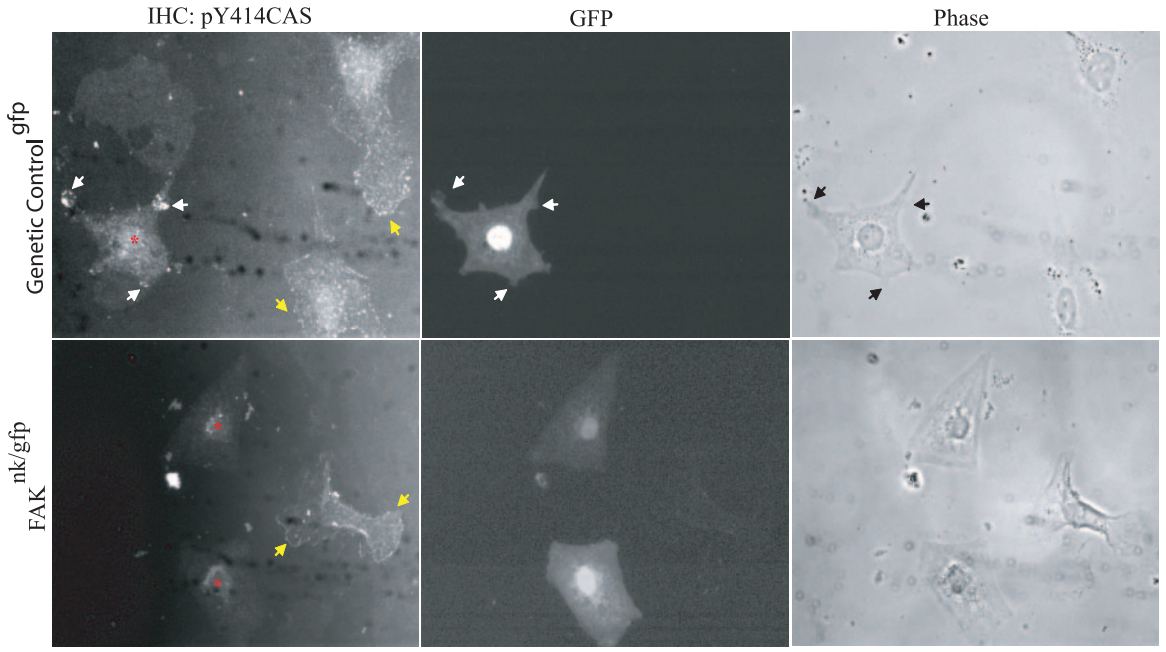

FIG. 8. FAK-null cardiomyocytes have reduced CAS phosphorylation. Cells were isolated from genetic control^{gfp} and FAK$^{nk/gfp}$ hearts and plated on fibronectin (10 μg/ml) as described in Materials and Methods. Cells were treated with PE for 30 min in serum-free medium. Cells were fixed, permeabilized, and stained with anti-phospho-Y414CAS antibody. The GFP channel is shown to aid in the identification of cardiomyocytes. Black or white arrows and yellow arrows indicate focal adhesion-like complexes at the periphery of lamellipodia in cardiomyocytes (*) and in fibroblasts, respectively. Data are representative of at least 100 cells in three separate experiments. IHC, immunohistochemistry.

targeted rescue approaches should prove useful in determining which (if any) of these additional cell types contribute to the cardiac phenotypes observed for the FAK^{nk} mice.

In mice, the superior and inferior cushions of the AV canal are formed by epithelial-to-mesenchymal transformation (EMT) at E10.5. The cushions fuse at E11.5 to E12.5 to form the valve primordia at E13.5 and undergo substantial remodeling until E17.5 to form the valve leaflets (11). The AV and OFT cushions in FAK^{nk} hearts appeared normal in size at E12.5 and valves were appropriately remodeled in most postnatal FAK^{nk} hearts, suggesting that EMT may not have been altered due to FAK deficiency. Subsequent to EMT, the OFT cushions undergo proliferation, fusion, invasion by NCCs (26, 32, 47), and myocardialization (45, 68), resulting in the formation of the spiral aorticopulmonary septum, the proximal OFT septum, and valves. Normally, myocardialization starts at E11.5 and continues to progress until the proximal outlet septum is completely muscularized by E15.5 (52). Abnormal myocardialization of the OFT has been associated with defects in the proximal OFT septum resulting in VSD accompanied by DORV in TGF-β2$^{-/-}$ and loop-tail (Lp) mice (2, 52). Myocardialization occurs mainly due to polarized myocyte movement (or chemotaxis) from the adjacent myocardium into the cushion tissue (52, 68); however, transdifferentiation of the mesenchymal cells to myocytes (regulated by signals from the myocytes that have already migrated into the cushions) also contributes to the process (19, 38, 67, 68).

A number of autocrine factors likely mediate myocyte chemotaxis in vivo. Members of the TGF-β superfamily (including TGF-β2 and Bmp4), the FGF family (FGF8 and FGF10), and the Wnt 5a and Wnt 11 ligands are thought to be particularly important in this regard, since disruption of pathways mediated by these factors leads to defective formation and remodeling of the OFT (14, 16, 27, 41, 43, 49). Herein, we have used a novel in vitro approach to quantify myocyte chemotaxis and have determined that FAK is necessary for optimal serum-induced cardiomyocyte motility. Future studies will be required to determine whether FAK interacts functionally or genetically with the motility signals induced by the aforementioned ligands.

Although appropriate cardiomyocyte migration is necessary for proper cardiac morphogenesis and may regulate cardiac repair following myocardial infarction (6), surprisingly little is known regarding the downstream signaling pathways that regulate myocyte motility either in vitro or in vivo. Chemotaxis occurs by a coordinated cyclical progression of four biomechanical events: cell polarization and membrane protrusion at the leading edge; construction and deconstruction of new focal adhesions; contraction of the cell body; and retraction of the trailing edge (54). It is becoming clear that activation of FAK and coordinated regulation of the small GTPases Cdc42, Rac, and Rho, which regulate cytoskeletal remodeling (cell adhesion, filopodial extensions, and membrane ruffles and cell contraction, respectively), in particular appear to play a central role in this dynamic process in many cell types (20, 51). Since FAK is activated in a polarized fashion and can drive the formation of a multiprotein signaling complex through protein-protein interactions, we hypothesized that recruitment/phosphorylation of a FAK binding partner is necessary for cells to respond in a polarized fashion to a chemotactic gradient. To this end, we found that CAS phosphorylation on Y414 was localized to peripheral lamellipodial structures in control myo-

cytes but not in FAK^{nk} myocytes. Since Y414 is a known Src phosphorylation site (57), it is likely that FAK is necessary for providing a scaffold for Src and CAS; however, it is possible that FAK may also contribute to the direct phosphorylation of this site. Since pY414 can direct binding of the adapter proteins CRK and CRKL (v-crk sarcoma virus CT10 oncogene homolog avian-like) to the focal adhesions to facilitate localized Rac activation and cell motility (13, 24, 31, 37, 40, 57), this could be one of the possible mechanisms that leads to impaired migration of FAK-null cardiomyocytes into the cushion tissue. In this regard, it is interesting to note that the focal adhesion protein CRKL maps within a 3-Mb region of chromosome 22q11 that is deleted in patients with DiGeorge syndrome and that CRKL-null mice phenocopy the cardiac defects, including VSD and DORV, observed for these patients (18, 43).

In addition to the modulation of the CAS/CRK second-messenger signaling pathways, FAK likely regulates the transmission of signals into the nucleus with resultant changes in gene expression. Our target gene analysis in FAK^{nk} hearts, where FAK deficiency was induced in *nkx2-5*-expressing cells, did not reveal aberrant expression of selected genes that are involved in ventricular septation and OFT development. Indeed, Tbx1, Tbx5, and TGF-β2 levels were not significantly different between genetic control and FAK^{nk} hearts. It is possible that the regional expression pattern may be altered without an accompanying change in the overall message; however, we have performed extensive in situ analysis of these target genes with FAK-depleted *Xenopus* embryos at various stages and have not observed a change in the expression levels or expression patterns of these genes (unpublished observations). Thus, our data indicate that these important regulatory genes may not be involved in the observed OFT defects and VSD in the FAK^{nk} mutants. However, future identification of FAK-dependent gene targets may lead to the discovery of novel factors that regulate ventricular septation.

In summary, we have selectively deleted FAK from *nkx2-5*-expressing cells during midgestation and determined that FAK is essential for appropriate ventricular septation and OFT alignment. The defects observed for the FAK^{nk} hearts resemble some of the most common congenital malformations in humans. The observed defects are consistent with abnormalities observed for polarized myocyte motility; thus, it is possible that appropriate closure of the interventricular foramen is dependent upon FAK-mediated myocyte migration into the proximal conal ridges. Future studies to determine the precise upstream and downstream FAK-dependent signals that regulate myocyte chemotaxis could lead to therapeutic advances in the treatment of CHD.

ACKNOWLEDGMENTS

We thank Kathleen Caron, Nadia Malouf, and Kumar Pandya (UNC-CH) for helpful advice and discussions during the preparation of the manuscript. The MF20 hybridoma antibody was obtained from the Developmental Studies Hybridoma Bank developed under the auspices of the NICHD and maintained by the University of Iowa, Department of Biological Sciences, Iowa City, IA 52242.

This work was supported in part by grants from NIH-NHLBI (HL-081844 and HL-071054) and the American Heart Association (AHA) (0355776U) to J.M.T., NIH-NHLBI (HL070953) and AHA (0555476U) to C.P.M., NS19090 to L.F.R., and HL71266 and HL49277 to O.S. J.W.H. was supported by AHA Fellow to Faculty Transition Award 0275023N.

REFERENCES

1. **Abu-Issa, R., G. Smyth, I. Smoak, K. Yamamura, and E. N. Meyers.** 2002. Fgf8 is required for pharyngeal arch and cardiovascular development in the mouse. Development **129:**4613–4625.
2. **Bartram, U., D. G. Molin, L. J. Wisse, A. Mohamad, L. P. Sanford, T. Doetschman, C. P. Speer, R. E. Poelmann, and A. C. Gittenberger-de Groot.** 2001. Double-outlet right ventricle and overriding tricuspid valve reflect disturbances of looping, myocardialization, endocardial cushion differentiation, and apoptosis in TGF-beta(2)-knockout mice. Circulation **103:**2745–2752.
3. **Beggs, H. E., D. Schahin-Reed, K. Zang, S. Goebbels, K. A. Nave, J. Gorski, K. R. Jones, D. Sretavan, and L. F. Reichardt.** 2003. FAK deficiency in cells contributing to the basal lamina results in cortical abnormalities resembling congenital muscular dystrophies. Neuron **40:**501–514.
4. **Benlimame, N., Q. He, S. Jie, D. Xiao, Y. J. Xu, M. Loignon, D. D. Schlaepfer, and M. A. Alaoui-Jamali.** 2005. FAK signaling is critical for ErbB-2/ErbB-3 receptor cooperation for oncogenic transformation and invasion. J. Cell Biol. **171:**505–516.
5. **Besson, W. T., III, M. L. Kirby, L. H. Van Mierop, and J. R. Teabeaut II.** 1986. Effects of the size of lesions of the cardiac neural crest at various embryonic ages on incidence and type of cardiac defects. Circulation **73:**360–364.
6. **Bock-Marquette, I., A. Saxena, M. D. White, J. M. Dimaio, and D. Srivastava.** 2004. Thymosin beta4 activates integrin-linked kinase and promotes cardiac cell migration, survival and cardiac repair. Nature **432:**466–472.
7. **Bouton, A. H., R. B. Riggins, and P. J. Bruce-Staskal.** 2001. Functions of the adapter protein Cas: signal convergence and the determination of cellular responses. Oncogene **20:**6448–6458.
8. **Brancaccio, M., L. Fratta, A. Notte, E. Hirsch, R. Poulet, S. Guazzone, M. De Acetis, C. Vecchione, G. Marino, F. Altruda, L. Silengo, G. Tarone, and G. Lembo.** 2003. Melusin, a muscle-specific integrin beta1-interacting protein, is required to prevent cardiac failure in response to chronic pressure overload. Nat. Med. **9:**68–75.
9. **Bronson, S. K., E. G. Plaehn, K. D. Kluckman, J. R. Hagaman, N. Maeda, and O. Smithies.** 1996. Single-copy transgenic mice with chosen-site integration. Proc. Natl. Acad. Sci. USA **93:**9067–9072.
10. **Cheresh, D. A., J. Leng, and R. L. Klemke.** 1999. Regulation of cell contraction and membrane ruffling by distinct signals in migratory cells. J. Cell Biol. **146:**1107–1116.
11. **Conway, S. J., A. Kruzynska-Frejtag, P. L. Kneer, M. Machnicki, and S. V. Koushik.** 2003. What cardiovascular defect does my prenatal mouse mutant have, and why? Genesis **35:**1–21.
12. **DiMichele, L. A., J. T. Doherty, M. Rojas, H. E. Beggs, L. F. Reichardt, C. P. Mack, and J. M. Taylor.** 2006. Myocyte-restricted focal adhesion kinase deletion attenuates pressure overload-induced hypertrophy. Circ. Res. **99:**636–645.
13. **Feller, S. M.** 2001. Crk family adaptors—signalling complex formation and biological roles. Oncogene **20:**6348–6371.
14. **Frank, D. U., L. K. Fotheringham, J. A. Brewer, L. J. Muglia, M. Tristani-Firouzi, M. R. Capecchi, and A. M. Moon.** 2002. An Fgf8 mouse mutant phenocopies human 22q11 deletion syndrome. Development **129:**4591–4603.
15. **Furuta, Y., D. Ilic, S. Kanazawa, N. Takeda, T. Yamamoto, and S. Aizawa.** 1995. Mesodermal defect in late phase of gastrulation by a targeted mutation of focal adhesion kinase, FAK. Oncogene **11:**1989–1995.
16. **Gaussin, V., T. Van de Putte, Y. Mishina, M. C. Hanks, A. Zwijsen, D. Huylebroeck, R. R. Behringer, and M. D. Schneider.** 2002. Endocardial cushion and myocardial defects after cardiac myocyte-specific conditional deletion of the bone morphogenetic protein receptor ALK3. Proc. Natl. Acad. Sci. USA **99:**2878–2883.
17. **Goddeeris, M. M., R. Schwartz, J. Klingensmith, and E. N. Meyers.** 2007. Independent requirements for Hedgehog signaling by both the anterior heart field and neural crest cells for outflow tract development. Development **134:**1593–1604.
18. **Guris, D. L., J. Fantes, D. Tara, B. J. Druker, and A. Imamoto.** 2001. Mice lacking the homologue of the human 22q11.2 gene CRKL phenocopy neurocristopathies of DiGeorge syndrome. Nat. Genet. **27:**293–298.
19. **Hagel, M., E. L. George, A. Kim, R. Tamimi, S. L. Opitz, C. E. Turner, A. Imamoto, and S. M. Thomas.** 2002. The adaptor protein paxillin is essential for normal development in the mouse and is a critical transducer of fibronectin signaling. Mol. Cell. Biol. **22:**901–915.
20. **Hakuno, D., T. Takahashi, J. Lammerding, and R. T. Lee.** 2005. Focal adhesion kinase signaling regulates cardiogenesis of embryonic stem cells. J. Biol. Chem. **280:**39534–39544.
21. **Hescheler, J., and B. K. Fleischmann.** 2000. Integrins and cell structure: powerful determinants of heart development and heart function. Cardiovasc. Res. **47:**645–647.
22. **Hoffman, J. I.** 1995. Incidence of congenital heart disease. I. Postnatal incidence. Pediatr. Cardiol. **16:**103–113.
23. **Hoffman, J. I.** 1995. Incidence of congenital heart disease. II. Prenatal incidence. Pediatr. Cardiol. **16:**155–165.
24. **Honda, A., M. Nogami, T. Yokozeki, M. Yamazaki, H. Nakamura, H.**

Watanabe, K. Kawamoto, K. Nakayama, A. J. Morris, M. A. Frohman, and Y. Kanaho. 1999. Phosphatidylinositol 4-phosphate 5-kinase alpha is a downstream effector of the small G protein ARF6 in membrane ruffle formation. Cell **99:**521–532.

25. **Honda, H., H. Oda, T. Nakamoto, Z. Honda, R. Sakai, T. Suzuki, T. Saito, K. Nakamura, K. Nakao, T. Ishikawa, M. Katsuki, Y. Yazaki, and H. Hirai.** 1998. Cardiovascular anomaly, impaired actin bundling and resistance to Src-induced transformation in mice lacking p130Cas. Nat. Genet. **19:**361–365.
26. **Hutson, M. R., and M. L. Kirby.** 2003. Neural crest and cardiovascular development: a 20-year perspective. Birth Defects Res. Part C **69:**2–13.
27. **Hutson, M. R., P. Zhang, H. A. Stadt, A. K. Sato, Y. X. Li, J. Burch, T. L. Creazzo, and M. L. Kirby.** 2006. Cardiac arterial pole alignment is sensitive to FGF8 signaling in the pharynx. Dev. Biol. **295:**486–497.
28. **Hynes, R. O.** 1992. Integrins: versatility, modulation, and signaling in cell adhesion. Cell **69:**11–25.
29. **Ilagan, R., R. Abu-Issa, D. Brown, Y. P. Yang, K. Jiao, R. J. Schwartz, J. Klingensmith, and E. N. Meyers.** 2006. Fgf8 is required for anterior heart field development. Development **133:**2435–2445.
30. **Ilic, D., Y. Furuta, S. Kanazawa, N. Takeda, K. Sobue, N. Nakatsuji, S. Nomura, J. Fujimoto, M. Okada, and T. Yamamoto.** 1995. Reduced cell motility and enhanced focal adhesion contact formation in cells from FAK-deficient mice. Nature **377:**539–544.
31. **Iwahara, T., T. Akagi, Y. Fujitsuka, and H. Hanafusa.** 2004. CrkII regulates focal adhesion kinase activation by making a complex with Crk-associated substrate, p130Cas. Proc. Natl. Acad. Sci. USA **101:**17693–17698.
32. **Kirby, M. L.** 1987. Cardiac morphogenesis—recent research advances. Pediatr. Res. **21:**219–224.
33. **Kirby, M. L., T. F. Gale, and D. E. Stewart.** 1983. Neural crest cells contribute to normal aorticopulmonary septation. Science **220:**1059–1061.
34. **Kirby, M. L., K. L. Turnage III, and B. M. Hays.** 1985. Characterization of conotruncal malformations following ablation of "cardiac" neural crest. Anat. Rec. **213:**87–93.
35. **Kirby, M. L., and K. L. Waldo.** 1995. Neural crest and cardiovascular patterning. Circ. Res. **77:**211–215.
36. **Kirby, M. L., and K. L. Waldo.** 1990. Role of neural crest in congenital heart disease. Circulation **82:**332–340.
37. **Klemke, R. L., J. Leng, R. Molander, P. C. Brooks, K. Vuori, and D. A. Cheresh.** 1998. CAS/Crk coupling serves as a "molecular switch" for induction of cell migration. J. Cell Biol. **140:**961–972.
38. **Kruithof, B. P., M. J. Van Den Hoff, S. Tesink-Taekema, and A. F. Moorman.** 2003. Recruitment of intra- and extracardiac cells into the myocardial lineage during mouse development. Anat. Rec. Part A **271:**303–314.
39. **Kuramochi, Y., X. Guo, and D. B. Sawyer.** 2006. Neuregulin activates erbB2-dependent src/FAK signaling and cytoskeletal remodeling in isolated adult rat cardiac myocytes. J. Mol. Cell. Cardiol. **41:**228–235.
40. **Li, L., D. L. Guris, M. Okura, and A. Imamoto.** 2003. Translocation of CrkL to focal adhesions mediates integrin-induced migration downstream of Src family kinases. Mol. Cell. Biol. **23:**2883–2892.
41. **Marguerie, A., F. Bajolle, S. Zaffran, N. A. Brown, C. Dickson, M. E. Buckingham, and R. G. Kelly.** 2006. Congenital heart defects in Fgfr2-IIIb and Fgf10 mutant mice. Cardiovasc. Res. **71:**50–60.
42. **Mohun, T., R. Orford, and C. Shang.** 2003. The origins of cardiac tissue in the amphibian, Xenopus laevis. Trends Cardiovasc. Med. **13:**244–248.
43. **Moon, A. M., D. L. Guris, J. H. Seo, L. Li, J. Hammond, A. Talbot, and A. Imamoto.** 2006. Crkl deficiency disrupts Fgf8 signaling in a mouse model of 22q11 deletion syndromes. Dev. Cell **10:**71–80.
44. **Moorman, A. F., and V. M. Christoffels.** 2003. Cardiac chamber formation: development, genes, and evolution. Physiol. Rev. **83:**1223–1267.
45. **Moralez, I., A. Phelps, B. Riley, M. Raines, E. Wirrig, B. Snarr, J. P. Jin, M. Van Den Hoff, S. Hoffman, and A. Wessels.** 2006. Muscularizing tissues in the endocardial cushions of the avian heart are characterized by the expression of h1-calponin. Dev. Dyn. **235:**1648–1658.
46. **Moses, K. A., F. DeMayo, R. M. Braun, J. L. Reecy, and R. J. Schwartz.** 2001. Embryonic expression of an Nkx2-5/Cre gene using ROSA26 reporter mice. Genesis **31:**176–180.
47. **Nishibatake, M., M. L. Kirby, and L. H. Van Mierop.** 1987. Pathogenesis of persistent truncus arteriosus and dextroposed aorta in the chick embryo after neural crest ablation. Circulation **75:**255–264.
48. **Olson, E. N.** 2004. A decade of discoveries in cardiac biology. Nat. Med. **10:**467–474.
49. **Park, E. J., L. A. Ogden, A. Talbot, S. Evans, C. L. Cai, B. L. Black, D. U. Frank, and A. M. Moon.** 2006. Required, tissue-specific roles for Fgf8 in outflow tract formation and remodeling. Development **133:**2419–2433.
50. **Parsons, J. T.** 2003. Focal adhesion kinase: the first ten years. J. Cell Sci. **116:**1409–1416.
51. **Parsons, J. T., K. H. Martin, J. K. Slack, J. M. Taylor, and S. A. Weed.** 2000. Focal adhesion kinase: a regulator of focal adhesion dynamics and cell movement. Oncogene **19:**5606–5613.
52. **Phillips, H. M., J. N. Murdoch, B. Chaudhry, A. J. Copp, and D. J. Henderson.** 2005. Vangl2 acts via RhoA signaling to regulate polarized cell movements during development of the proximal outflow tract. Circ. Res. **96:**292–299.
53. **Pierpont, M. E., R. R. Markwald, and A. E. Lin.** 2000. Genetic aspects of atrioventricular septal defects. Am. J. Med. Genet. **97:**289–296.
54. **Ridley, A. J., M. A. Schwartz, K. Burridge, R. A. Firtel, M. H. Ginsberg, G. Borisy, J. T. Parsons, and A. R. Horwitz.** 2003. Cell migration: integrating signals from front to back. Science **302:**1704–1709.
55. **Schroeder, J. A., L. F. Jackson, D. C. Lee, and T. D. Camenisch.** 2003. Form and function of developing heart valves: coordination by extracellular matrix and growth factor signaling. J. Mol. Med. **81:**392–403.
56. **Shai, S. Y., A. E. Harpf, C. J. Babbitt, M. C. Jordan, M. C. Fishbein, J. Chen, M. Omura, T. A. Leil, K. D. Becker, M. Jiang, D. J. Smith, S. R. Cherry, J. C. Loftus, and R. S. Ross.** 2002. Cardiac myocyte-specific excision of the beta1 integrin gene results in myocardial fibrosis and cardiac failure. Circ. Res. **90:**458–464.
57. **Shin, N. Y., R. S. Dise, J. Schneider-Mergener, M. D. Ritchie, D. M. Kilkenny, and S. K. Hanks.** 2004. Subsets of the major tyrosine phosphorylation sites in Crk-associated substrate (CAS) are sufficient to promote cell migration. J. Biol. Chem. **279:**38331–38337.
58. **Shubeita, H. E., J. Thorburn, and K. R. Chien.** 1992. Microinjection of antibodies and expression vectors into living myocardial cells. Development of a novel approach to identify candidate genes that regulate cardiac growth and hypertrophy. Circulation **85:**2236–2246.
59. **Srivastava, D.** 2001. Genetic assembly of the heart: implications for congenital heart disease. Annu. Rev. Physiol. **63:**451–469.
60. **Srivastava, D., and E. N. Olson.** 2000. A genetic blueprint for cardiac development. Nature **407:**221–226.
61. **Tachibana, K., T. Urano, H. Fujita, Y. Ohashi, K. Kamiguchi, S. Iwata, H. Hirai, and C. Morimoto.** 1997. Tyrosine phosphorylation of Crk-associated substrates by focal adhesion kinase. A putative mechanism for the integrin-mediated tyrosine phosphorylation of Crk-associated substrates. J. Biol. Chem. **272:**29083–29090.
62. **Tan, S. S., and G. Morriss-Kay.** 1985. The development and distribution of the cranial neural crest in the rat embryo. Cell Tissue Res. **240:**403–416.
63. **Taylor, J. M., C. P. Mack, K. Nolan, C. P. Regan, G. K. Owens, and J. T. Parsons.** 2001. Selective expression of an endogenous inhibitor of FAK regulates proliferation and migration of vascular smooth muscle cells. Mol. Cell. Biol. **21:**1565–1572.
64. **Taylor, J. M., J. D. Rovin, and J. T. Parsons.** 2000. A role for focal adhesion kinase in phenylephrine-induced hypertrophy of rat ventricular cardiomyocytes. J. Biol. Chem. **275:**19250–19257.
65. **Vadlamudi, R. K., A. A. Sahin, L. Adam, R. A. Wang, and R. Kumar.** 2003. Heregulin and HER2 signaling selectively activates c-Src phosphorylation at tyrosine 215. FEBS Lett. **543:**76–80.
66. **Valencik, M. L., R. S. Keller, J. C. Loftus, and J. A. McDonald.** 2002. A lethal perinatal cardiac phenotype resulting from altered integrin function in cardiomyocytes. J. Card. Fail. **8:**262–272.
67. **van den Hoff, M. J., B. P. Kruithof, A. F. Moorman, R. R. Markwald, and A. Wessels.** 2001. Formation of myocardium after the initial development of the linear heart tube. Dev. Biol. **240:**61–76.
68. **van den Hoff, M. J., A. F. Moorman, J. M. Ruijter, W. H. Lamers, R. W. Bennington, R. R. Markwald, and A. Wessels.** 1999. Myocardialization of the cardiac outflow tract. Dev. Biol. **212:**477–490.
69. **Vartanian, T., A. Goodearl, S. Lefebvre, S. K. Park, and G. Fischbach.** 2000. Neuregulin induces the rapid association of focal adhesion kinase with the erbB2-erbB3 receptor complex in Schwann cells. Biochem. Biophys. Res. Commun. **271:**414–417.
70. **von Both, I., C. Silvestri, T. Erdemir, H. Lickert, J. R. Walls, R. M. Henkelman, J. Rossant, R. P. Harvey, L. Attisano, and J. L. Wrana.** 2004. Foxh1 is essential for development of the anterior heart field. Dev. Cell **7:**331–345.
71. **Vuori, K., and E. Ruoslahti.** 1995. Tyrosine phosphorylation of p130Cas and cortactin accompanies integrin-mediated cell adhesion to extracellular matrix. J. Biol. Chem. **270:**22259–22262.
72. **Waldo, K. L., D. Kumiski, and M. L. Kirby.** 1996. Cardiac neural crest is essential for the persistence rather than the formation of an arch artery. Dev. Dyn. **205:**281–292.
73. **Xu, H., M. Morishima, J. N. Wylie, R. J. Schwartz, B. G. Bruneau, E. A. Lindsay, and A. Baldini.** 2004. Tbx1 has a dual role in the morphogenesis of the cardiac outflow tract. Development **131:**3217–3227.
74. **Yang, J. T., B. L. Bader, J. A. Kreidberg, M. Ullman-Cullere, J. E. Trevithick, and R. O. Hynes.** 1999. Overlapping and independent functions of fibronectin receptor integrins in early mesodermal development. Dev. Biol. **215:**264–277.
75. **Zaffran, S., and M. Frasch.** 2002. Early signals in cardiac development. Circ. Res. **91:**457–469.
76. **Zeisberg, E. M., Q. Ma, A. L. Juraszek, K. Moses, R. J. Schwartz, S. Izumo, and W. T. Pu.** 2005. Morphogenesis of the right ventricle requires myocardial expression of Gata4. J. Clin. Investig. **115:**1522–1531.
77. **Zhang, Z., F. Cerrato, H. Xu, F. Vitelli, M. Morishima, J. Vincentz, Y. Furuta, L. Ma, J. F. Martin, A. Baldini, and E. Lindsay.** 2005. Tbx1 expression in pharyngeal epithelia is necessary for pharyngeal arch artery development. Development **132:**5307–5315.